Radiocarbon, Vol 62, Nr 2, 2020, p 379–401 DOI:10.1017/RDC.2020.3

BAYESIAN MODELING OF WOOD-AGE OFFSETS IN CREMATED BONE

Helene Agerskov Rose[1]* • John Meadows[1,2] • Mogens Bo Henriksen[3]

[1]Foundation of Museums of the State of Schleswig-Holstein – Centre for Baltic and Scandinavian Archaeology, Schleswig, Schleswig-Holstein, Germany
[2]Christian-Albrechts-Universität zu Kiel – Leibniz-Laboratory for AMS Dating and Stable Isotope Research, Kiel, Schleswig-Holstein, Germany
[3]Odense City Museums – Archaeology, DK-5000 Odense C, Denmark

ABSTRACT. Experimental studies have shown that significant carbon exchange occurs between bone-apatite and the pyre atmosphere during cremation, which can cause a calendar date offset between the radiocarbon (^{14}C) event and the date of cremation. There are limited empirical data available to assess the magnitude of such wood-age offsets, but the aim of this paper is to test if they can be modeled statistically. We present new ^{14}C dates on modern bone cremated in realistic open-air experiments and on archaeological samples of cremated bone and associated organic material. Experimental results demonstrate a wide range of carbon exchange with a mean of 58.6 ± 14.8%. Archaeological results indicate that the wood-age offsets have an approximately exponential distribution. We test whether the default Charcoal Outlier_Model in OxCal v4.3, developed to reduce the impact of wood-age offsets in dates of charcoal, is appropriate for cremated bone, but find that it slightly underestimates apparent offsets. To counter the intrinsic age of both pyre fuel and unburned bio-apatite, we instead propose a bespoke Cremation Outlier_Model, which combines an exponential distribution of calendar age offsets with a minimum offset, and provides better estimates of the actual dates of cremations.

KEYWORDS: Bayesian modeling, cremated bone, experimental archaeology, outlier modeling, wood-age offset.

INTRODUCTION

Experimental studies (Zazzo et al. 2009, 2012; Hüls et al. 2010; Van Strydonck et al. 2010) have shown that only a fraction of original bone apatite carbon remains in the bone after cremation, but that there is a significant carbon uptake from the pyre atmosphere, which is derived mainly from the burning fuel. This was not realized almost two decades ago when a pioneering study on radiocarbon (^{14}C) dating cremated bone (CB) demonstrated that dates on the bio-apatite of fully calcined bone were comparable to those on associated charcoal (Lanting et al. 2001). As other studies tested the validity of dating CB using charcoal and other contemporaneous organic materials, they obtained similar results, and cases of charcoal dates being older than their associated CB were attributed to the "old-wood effect" (Lanting et al. 2001; De Mulder et al. 2009). Research continue investigating what isotopic changes bone undergoes when cremated (Van Strydonck et al. 2005, 2010; Naysmith et al. 2007; Olsen et al. 2008; Zazzo et al. 2009; Snoeck et al. 2016a). Experimental studies on the origin of CB apatite carbon demonstrated that bone exchanges carbon with the combustion atmosphere during cremation, giving calcined bone a mixed carbon signal. Hüls et al. (2010) cremated modern bone in a sealed furnace filled with ^{14}C-free CO_2 obtained from fossil fuel, and by dating the CB found that 53–86% of carbon in re-crystallized bio-apatite was derived from the cremation atmosphere. This was confirmed by open-air experiments under natural conditions, where Zazzo et al. (2012) using archaeological bone and recent wood measured a carbon exchange of 48–91%, while Snoeck et al. (2014), using modern bone and old wood of known-age, measured a carbon exchange of 39–95%. Carbon exchange between the bone and the combustion atmosphere will cause a calendar date offset between the calibrated ^{14}C measurement and the main event of interest (the date of cremation), which we will in the present paper refer to as a wood-age offset.

*Corresponding author. Email: helene.rose@zbsa.eu

Unless a body is cremated with recent, short-lived fuel, the wood-age offset will always make the CB date older than original unburned bio-apatite. From an archaeological perspective, cremation is a separate event occurring after death and before burial, but they are here regarded as the same event, as their total duration is shorter than the resolution of the ^{14}C calibration curve for the Holocene (true in most but not all cultures). However, what is dated is a ^{14}C event, i.e. when atmospheric CO_2 is sequestered as organic carbon in a living organism, and the time over which this occurs (i.e. from formation to death) is here defined as the intrinsic age (IA) of any given material. We note that unburned bio-apatite also has an unknown IA, which may vary between individuals (depending on e.g. their age at death) and between bones of the same individual (due to differences in bio-apatite remodeling rates). Beside a lack of empirical data on bio-apatite remodeling rates, both age-at-death and skeletal element sampled are more difficult to determine in cremations than in inhumation burials. Nevertheless, given expected mortality patterns, we assume that the IA of unburned bio-apatite in prehistoric cremations seldom exceeds 1–2 decades.

The Importance of Fuel

The consequence of carbon exchange taking place between the bone and the pyre atmosphere is that dating CB is equivalent to or at least close to directly dating the fuel used on the pyre. If the pyre wood has a low IA, even a high degree of carbon exchange will lead to limited wood-age offsets, but conversely even low degrees of carbon exchange may cause significant wood-age offsets if the wood has a high IA. Another possible scenario is that the IA of fuel and bone may be close, causing constant CB ^{14}C ages, regardless of the degree of carbon exchange. It has long been recognized that charcoal might have a high IA, making the chronological relationship between the sample and the context from which it is recovered difficult to interpret (Bayliss 1999). There is however little information about the IA of the vast majority of archaeological charcoal samples, which is not only problematic when wood-age offsets are transferred to CB, but also when charcoal is used as known-age reference material.

It is clear that the choice of pyre wood is of concern when ^{14}C dating CB. Modern open-air experiments indicate cremation of a human body takes 5–7 hr and requires 1–2 m^3 of firewood, but with large variation dependent on wood type and quality, weather conditions, maintenance of the fire, etc. (Henriksen 2016). Prehistoric cremation graves are abundant worldwide, but actual pyre sites are rarely located, leaving only limited information on processes prior to interment, e.g. fuel procurement strategies and pyrotechnical operations of a cremation pyre. Even when pyre sites are located, they hold limited information, as the cremation process will have destroyed most of the fuel. Moreover, anthracological studies of pyre charcoal often only identify the wood taxa, without discussing wood-age. Hornstrup et al. (2005) analyzed charcoals from 16 cremation graves from Late Bronze Age to Early Iron Age in North and West Jutland showing a predominance of oak (75% *Quercus* sp.), followed by pine (25% *Pinus* sp.), alder (12.5% *Alnus* sp.), birch (12.5% *Betula* sp.), hazel (12.5% *Corylus* sp.) and willow (6% *Salix* sp.). Heather (*C. vulgaris*) was present in low frequencies in the majority of cremation graves at Hellegård in Central Jutland, demonstrating the practice of maintaining heath plains in the area. A similar distribution of wood species was used at contemporaneous settlement sites in the area, probably reflecting the local vegetation, but with a clear preference for oak. Although it requires seasoning for a few years, oak wood can produce long-lasting fires with high temperatures, and was widely used as a funerary fuel (e.g. Hissel et al. 2007; Henriksen 2009; Moskal-del Hoyo 2012; O'Donnell 2016; Martín-Seijo and César Vila 2018; Henriksen 2019). Anthracological studies of charcoal

https://doi.org/10.1017/RDC.2020.3 Published online by Cambridge University Press

from prehistoric burial and settlement sites in Denmark show a fuel procurement strategy with a preference for gathering deadwood with limited branch diameters, whereas actual production of fire wood was a later phenomenon associated with the establishment of towns in a time when cremation was no longer practiced (Hornstrup et al. 2005).

In this paper we analyze archaeological material from Aarre urnfield cemetery in West Jutland, Denmark. The archaeobotanical analyses of material from 11 urn graves at Aarre show a dominance of oak charcoal, followed by alder and maple (*Acer* sp.) (Online Supplementary Information 3, Effenberger 2017a, 2017b, 2019), corresponding well to the expected taxonomic availability in the area (Iversen 1974). All elements of the trees are represented, from twig to heartwood, with no apparent differences between graves. There would have been few oak trees in the open landscape around Aarre and wood gathering must have extended beyond the immediate surroundings (Iversen 1974). Alder is surprisingly common, given that it produces little heat and does not burn for long, but this may reflect the local abundance of the species. All elements of the trees were used, possibly reflecting gathering of deadwood or felling of younger trees, creating a combination of low IA for the young wood and IA ranging from $\geq$ 50 and up to 80 yr for alder and probably up to a few centuries for oak. Small caliber wood might have been used as kindling material, but might also reflect a landscape with few larger trees (Iversen 1974). The strategies for wood procurement at Aarre were probably determined by a combination of different factors, where wood availability both in close proximity and beyond seems to have played a large role.

Approaching the Issue of Wood-Age Offsets

There is limited empirical data available on the scale of wood-age offsets in CB, although multiple studies report ^{14}C dates on paired CB and charcoal (e.g. Lanting et al. 2001; Van Strydonck et al. 2005; Olsen et al. 2008; De Mulder et al. 2009; Chatters et al. 2017). As charcoal can be affected by variable wood-age offsets, it is difficult to infer what offset is transferred from the cremation fuel to the CB. To assess the scale of wood-age offsets in CB, it is desirable to focus on associated material with no IA, e.g. charred twigs or cereal grains, but such samples are often difficult to obtain from an archaeological context. Olsen et al. (2008) reported five pairs of ^{14}C dates on CB and pitch (wood resin with negligible IA) from the Danish Bronze Age, with a mean difference (CB – pitch ^{14}C age) of 26 ± 26 ^{14}C yr (ranging from 8 to 92 yr). In another paper, two combined CB ^{14}C ages were compared to a dendrochronological date, indicating that the CB was 73 ± 26 ^{14}C yr older than the date of cremation (Olsen et al. 2013). In a recent study of a historically attested Buddhist monk from medieval Japan, Minami et al. (2019) ^{14}C dated three samples of fully cremated white bone and a combination of the dates shows them to correspond well with the lifetime of the monk. As wood-age offsets are on the calendar scale ("type t" offsets: Bronk Ramsey 2009b), we calibrate these dates before comparing them using the Difference function in OxCal v4.3 (Bronk Ramsey 2009a). We model all the differences from Olsen et al. (2008; 2013) and Minami et al. (2019) in a bounded phase starting at zero (i.e. requiring the CB to have a wood-age offset) and summarize the now-constrained wood-age offsets using the KDE_Plot function (Bronk Ramsey 2017). Assuming an exponential distribution of wood-age offsets (i.e. applying a Tau_Boundary (Bronk Ramsey 2009a) to the end of the bounded phase), the posterior estimates of the offsets have a 22 yr median and a 1-σ range of 32 yr (Online Supplementary Information 1, Part 1). Based on this limited empirical data set, wood-age offsets in CB appear to be relatively small.

https://doi.org/10.1017/RDC.2020.3 Published online by Cambridge University Press

When bone is cremated, isotopic fractionation of carbon takes place as a function of time and temperature (Olsen et al. 2008; Zazzo et al. 2009), which in effect means there are no proxies available (e.g. $\delta^{13}C$ values) for assessing the scale of wood-age offsets in individual CB samples. Because of this, ^{14}C dates on CB are sometimes used as simple *termini post quem*, but this means discarding information about the dates of cremations and will be close to useless in cases where only CB dates are available. We propose to instead handle CB dates statistically using the Outlier_Model function of OxCal v4.3 (Bronk Ramsey 2009b)(OM), which allows dates to be weighted according to a prior probability for how likely they are to be misleading, and allows the user to specify a distribution for potential offsets. Calendar age offsets in samples susceptible to IA, e.g. charcoal from trunk wood, are assumed to approximately follow an exponential probability density function, i.e. most samples will date close to the event in question, but a diminishing number of dates will be increasingly older (Nicholls and Jones 2001; Dee and Bronk Ramsey 2014). This assumption can be modeled using the default Charcoal OM (Bronk Ramsey 2009b; Dee and Bronk Ramsey 2014), developed to reduce the impact of wood-age offsets in dates of charcoal, and it has been suggested to also apply this with varying scales to ^{14}C dates on CB (Garrow et al. 2014; Fitzpatrick et al. 2017). We will in this study take a step back and empirically investigate the scale of wood-age offsets and their underlying distribution, before finally proposing a suitable OM for ^{14}C dates on CB.

MATERIAL AND METHODS

Archaeological Material

CB and context associated organic samples were selected from an archaeological site in West Jutland, Denmark. Aarre urnfield cemetery (sandy soil with low carbonate levels, ca. 8°dH) is a large and well-documented site, with originally up to ca. 1000 burials. The cremated human remains were interred in funerary urns and covered by small earthen mounds enclosed by a ditch. A minority of the graves contained metal artifacts, which can be approximately dated by seriation of typological traits (Becker 1961; Jensen 1996). No cremation pyres have been located in the area and all graves are secondary deposits (Lorange 2015). Samples from 10 graves were selected for this study, comprising CB, charcoal and other charred plant material. The graves were excavated over the last decade and the contents of the cremation urns were excavated in a controlled indoor environment. Charcoal is interpreted as remains of pyre fuel, whereas cereal grains and seeds might have accompanied the deceased on the pyre. Grass (stems and a bulb of *Arrhenatherum elatius* ssp. *bulbosum*) and stems of heather (*Calluna vulgaris)* probably came from the area underneath or surrounding the pyre, and might have been used as kindling material, but might also have an altogether unintentional relationship to the cremation (Roehrs et al. 2013). All charcoal dates are susceptible to IA, and individual wood-age offsets were therefore estimated based on the typical lifespan of the species and the sampled section of the plant (e.g. trunk wood or twig).

Experimental Material

The third author carried out four separate open-air cremation experiments over the period 2014–2017, cremating modern animal bone using either recent wood or old wood of known age. The experiments took place in the author's garden on Funen in central Denmark. They were designed to mimic a prehistoric cremation pyre, albeit in a scaled down version, and did not allow close control of environmental parameters. Comparable amounts of bone and wood (ca. 6–7 kg wood per pyre) were burned in an iron brazier, which protected the

https://doi.org/10.1017/RDC.2020.3 Published online by Cambridge University Press

Table 1 Pyre fuel for experimental pyres with dendro dates and values of $F^{14}C$ and ^{14}C age (Hua et al. 2013; Levin et al. 2013; Reimer et al. 2013; Hammer and Levin 2017).

Pyre	Fuel	Dendro date	$F^{14}C$	^{14}C age
No. 8	Recent wood (*Fraxinus* sp.)	AD 1986–2013	1.0954 ± 0.0032	–729 ± 24
No. 9	Old wood (*Quercus* sp.)	AD 1100–1282	0.8987 ± 0.0013	858 ± 11
No. 11	As pyre no. 8	—	—	—
No. 16	Old wood (*Quercus* sp.)	AD 34–251	0.7926 ± 0.0017	1867 ± 14

Table 2 Animal bone for experimental pyres with slaughter dates and values of $F^{14}C$ and ^{14}C years. 2017 values are extrapolated from the ^{14}C activity of the previous decade (Hua et al. 2013; Levin et al. 2013; Hammer and Levin 2017).

Pyre	Bone	Slaughter date	$F^{14}C$	^{14}C age
No. 8	Sheep (*Ovis aries*), single cut of a hind limb	2013	1.0231 ± 0.0018	–183 ± 14
No. 9	Cattle (*Bos taurus*), single cut of a large diaphysis	2013	1.0231 ± 0.0018	–183 ± 14
No. 11	Sheep (*Ovis aries*), single cut of a hind limb	2015	1.0133 ± 0.0019	–106 ± 15
	Cattle (*Bos taurus*), single cut of a large diaphysis	2013	1.0231 ± 0.0018	–183 ± 14
No. 16	Sheep (*Ovis aries*), single cut of a hind limb	2017	1.0062 ± 0.0013	–50 ± 10

fire from the wind and ensured the bones were in close contact with the fuel until the fires burned down after 2–2.5 hr. Beyond igniting the fires, no additional wood was added (Henriksen 2016). Snoeck et al. (2014) conducted similar experiments, albeit with fleshed modern bone. The new contribution of our experiment is the dating of multiple bone fragments from the same bone, from the same pyre, thereby documenting variable uptake of exogenous carbon during cremation.

Pyres no. 8 and no. 11 used recent wood and pyres no. 9 and no. 16 used old dendro-dated wood (Table 1) (Daly 2011; Daly 2014). To obtain $F^{14}C$ values and ^{14}C ages for the old wood, the mean was calculated of the raw curve points over the dendro-dated growth periods (pyre no. 9: 850–670 cal BP, pyre no. 16: 1915–1700 cal BP) in the IntCal13 Northern Hemisphere atmospheric ^{14}C data set (Reimer et al. 2013). For the recent wood, data from the Bomb13NH1 (AD1650–2010) calibration curve (Hua et al. 2013) was combined with additional data points from the Hammer and Levin datasets of atmospheric ^{14}C activity from Jungfraujoch in the Swiss Alps (Online Supplementary Information 4) (Levin et al. 2013; Hammer and Levin 2017). Wood will have an inhomogeneous ^{14}C signal, but our approach effectively assumes that it was fully homogenized by combustion, and any differences in CB ^{14}C ages from each pyre are therefore due to differential carbon exchange. Cuts of cattle (*Bos taurus*) and sheep (*Ovis aries*) reared in Denmark were cooked and defleshed prior to cremation (Table 2). Although we assume that prehistoric humans were not defleshed before cremation, skin and flesh will combust at

https://doi.org/10.1017/RDC.2020.3 Published online by Cambridge University Press

lower temperatures before bio-apatite recrystallization occurs (Zazzo et al. 2009; Snoeck et al. 2014). Collagen from the bones themselves might however contribute to the carbon composition of the pyre atmosphere, but must be burnt out before recrystallization can begin, and should therefore have little effect on the CB ^{14}C age. The animals were all young specimens, so the slaughter dates are compared with recent measurements of atmospheric ^{14}C activity to obtain values of $F^{14}C$ and ^{14}C age before cremation (Levin et al. 2013; Hammer and Levin 2017). No measurements are yet available for 2017, but because the decline in atmospheric ^{14}C in recent years was relatively steady, we extrapolate a value from the trend over the previous decade. ^{14}C units were converted using Stuiver and Polach (1977), but as we report post-bomb ^{14}C data indicative of ^{14}C activity of the atmosphere rather than radioactive decay, we use the $F^{14}C$ convention rather than pMC (Reimer et al. 2004).

Laboratory Methods

Only samples of white CB were selected. To confirm they were fully calcined, aliquots of powdered untreated CB were analyzed by Fourier-transform infrared spectroscopy (FTIR). The crystallinity index (CI) was estimated as the splitting factor between the two absorption bands at ca. 603 and ca. 565 cm^{-1} ($CI = (A_{603} + A_{565})/A_{valley}$) (Person et al. 1995; Olsen et al. 2008). CB samples were sent to the Centre for Isotope Research (CIO) in Groningen, the Leibniz Laboratory (KIA) in Kiel and the Laboratory for Radiocarbon Dating (RICH) in Brussels for ^{14}C dating. As part of a comparison study, two CB samples were replicated between CIO and KIA; they were pretreated in Groningen following the CIO protocol, but were subsequently converted to CO_2 and dated in Kiel (Rose et al. 2019). It has been suggested that it may be unnecessary to bleach CB samples with e.g. sodium hypochlorite to remove any organic material (Snoeck et al. 2016b), but Groningen maintains the procedure as initially introduced by Lanting et al. (2001). Samples of context-associated organic material were sent for archaeobotanical analysis (Effenberger 2017a, 2017b, 2019) and identified single fragments were ^{14}C dated in Brussels or Kiel.

Pretreatment and Combustion

Samples of charred organics were extracted in Kiel and Brussels following standard acid–alkali–acid procedures (Grootes et al. 2004; Boudin et al. 2015). Samples of CB were extracted using different pretreatment procedures at the three laboratories (Rose et al. 2019). Brussels leached ca. 30% by weight of each solid CB sample in 1% hydrochloric acid, before it was powdered and treated with 1% acetic acid (24 hr) to remove calcite (Van Strydonck et al. 2009). Kiel crushed each CB sample before treating it with 0.6% acetic acid (5 × 30 min) and leaching ca. 50% with 1% hydrochloric acid (Hüls et al. 2010). Groningen treated CB samples with 1.5% sodium hypochlorite (48 hr, 20°C), followed by 6% (1M) acetic acid (24 hr, 20°C) (Dee et al. 2019). Kiel hydrolyzed two aliquots of the extracted apatite for five CB samples to increase measurement precision. All CB extracts were reacted with phosphoric acid to produce CO_2 and combusted to remove sulfur compounds.

Graphitization and AMS Measurement

Purified CO_2 of charred organics and CB was reduced to graphite for AMS measurement. Measurements in Brussels were performed on a Micadas (195.5 kV) AMS system (Boudin et al. 2015). Kiel used a HVEE 3 MV Tandetron 4130 AMS system (Nadeau et al. 1997) and Groningen used a Micadas (180 kV) AMS system (Dee et al. 2019). The laboratories corrected the resulting ^{14}C-contents for fractionation using the simultaneously AMS-measured $^{14}C/^{12}C$ and $^{13}C/^{12}C$ isotope ratios (Stuiver and Polach 1977).

https://doi.org/10.1017/RDC.2020.3 Published online by Cambridge University Press

Calculating Carbon Exchange

^{14}C ages of CB have been shown to plot along or close to a mixing line between the end-members unburned apatite and burning atmosphere ($CO_{2\ AIR} + CO_{2\ FUEL}$) (Hüls et al. 2010; Zazzo et al. 2012). Bone organic matter does not contribute to the CB carbon signal, as it degrades at lower temperatures before apatite recrystallization takes place (Zazzo et al. 2009; Snoeck et al. 2014). The percent carbon exchange between unburned apatite and the pyre atmosphere, as indicated by $F^{14}C$, can be calculated using mass balance Equation (1), assuming the $F^{14}C$ content to be evenly distributed throughout the wood and animals.

$$\%carbon\ exchange = \frac{F^{14}C_{\text{unburned apatite}} - F^{14}C_{CB}}{F^{14}C_{\text{unburned apatite}} - F^{14}C_{\text{pyre atmosphere}}} * 100(\%) \quad (1)$$

Where $F^{14}C_{\text{unburned apatite}}$ is the atmospheric $F^{14}C$ when the animal was slaughtered, $F^{14}C_{CB}$ is the $F^{14}C$ concentration in cremated bone, and $F^{14}C_{\text{pyre atmosphere}}$ is the mean $F^{14}C$ over the period of wood growth, as it will be dominated by CO_2 generated by the wood combustion (Tables 1 and 2) (Zazzo et al. 2012). % carbon exchange uncertainties for individual samples can be calculated using Equation (2), where σ_{bone} is the uncertainty in unburned apatite $F^{14}C$, σ_{CB} is the uncertainty in cremated bone $F^{14}C$, σ_{fuel} is the uncertainty in wood (fuel) $F^{14}C$, and $F^{14}C_{CB}$ is the $F^{14}C$ concentration in cremated bone. The uncertainties are however relatively trivial (ca. ± 0.5%) compared to the observed range of values.

$$\%uncertainty = \frac{\sqrt{\sigma_{\text{bone}}{}^2 + \sigma_{CB}{}^2 + \sigma_{\text{bone}}{}^2 + \sigma_{\text{fuel}}{}^2}}{F^{14}C_{CB}} * 100(\%) \quad (2)$$

RESULTS

Archaeological Dataset

We report a total of 43 AMS dates measured on 36 unique samples from 10 individual urnfield graves (Table 3). These include measurements on CB, charcoal and short-lived charred plant material (cereal grains and fragments of grass). CI values of CB are all acceptable (>5) and CB $\delta^{13}C$ values (mean = –23.2 ± 1.9 $\delta^{13}C$) and %C (mean = 0.19 ± 0.09 %C) fall within expected ranges. Values of $\delta^{13}C$ are measured by AMS and the results will be affected by fractionation during acid extraction, graphitization and AMS measurement. Also %C is not strictly comparable between laboratories, as pretreatment methods vary and %C is calculated at different steps in the process (Rose et al. 2019). Archaeobotanical results are provided in Online Supplementary Information 3.

AMS dates are calibrated in OxCal v4.3 using the IntCal13 calibration curve (Bronk Ramsey 2009a; Reimer et al. 2013) and differences between context associated material and CB are calculated (Figure 1, Online Supplementary Information 1, Part 2). As expected, differences cluster around zero (indicated by the vertical line), but are strongly skewed towards positive values, i.e. associated samples often date older than the CB. The large majority of charcoal samples are much older than the CB dates, however, and might be derived from residual material relating to documented extensive Bronze Age activities in the area (Lorange 2015), notwithstanding the excavation of these urns under laboratory conditions. The pyre site or sites have not been located and there is no information on whether a new area was used for each pyre, or whether the same area was used repeatedly. It is possible that some pyres have been constructed on top of older cooking pits from the Bronze Age.

https://doi.org/10.1017/RDC.2020.3 Published online by Cambridge University Press

Table 3 Radiocarbon results on the archaeological data set from Aarre urnfield cemetery (West Jutland, Denmark). Replicate measurements have been tested for consistency and combined following Ward and Wilson (1978).

Context	Lab code	Sample ID	Material	CI	%C of extract	Corrected pMC	AMS $\delta^{13}C$ (‰VPDB)[1]	^{14}C age (BP)
Grave A86, urn	KIA-53941	x339	*Acer* sp. trunk wood charcoal (Ø > 10 cm)	—	63.96	73.60 ± 0.23	–25.3	2463 ± 25
	KIA-53942	x340	Cremated bone (human)	5.4	0.35	74.37 ± 0.24	–19.7	2379 ± 26
	KIA-53942	X340	Cremated bone (human), replicate	—	—	74.31 ± 0.23	–22.8	2385 ± 25
Weighted mean: sample x340, T' = 0.0, T' (5%) = 3.8, v = 1, 2382 ± 19 BP								
Grave A95, pit	KIA-53984	x368 no.1	*Quercus* sp. twig charcoal (Ø < 0.3 cm)	—	70.68	74.45 ± 0.23	–28.4	2370 ± 25
	KIA-53985	x368 no.3	*Acer* sp. twig charcoal (Ø < 0.5 cm)	—	70.49	73.90 ± 0.23	–27.7	2430 ± 26
Grave A95, urn	RICH-25342	x369	Cremated bone (human)	7.8	0.11	73.90 ± 0.25	–24.3	2428 ± 27
Grave A99, pit	RICH-25071	x65 no.2	*Alnus* sp. trunk wood charcoal (Ø 8-10 cm)	—	60.00	75.39 ± 0.28	–33.3	2269 ± 29
	RICH-25067	x65 no.3	*Quercus* sp. trunk wood charcoal (Ø < 10 cm)	—	61.00	67.85 ± 0.26	–31.6	3115 ± 31
Grave A99, urn	GrM-16774	x345	Cremated bone (human)	6.5	0.06	75.50 ± 0.17	–26.5	2255 ± 20
	RICH-25069	x346 no.1	*Alnus* sp. twig charcoal (Ø < 0.3 cm)	—	53.50	77.14 ± 0.28	–31.8	2085 ± 29
	RICH-25066	x346 no.27	Alnus sp. trunk wood charcoal (Ø > 10 cm)	—	61.60	75.56 ± 0.28	–35.3	2251 ± 30
Grave A117, urn	GrM-14604[2]	x762	Cremated bone (human)	6.0	0.10	73.75 ± 0.13	–25.7	2445 ± 20
	KIA-53098[2]	x762	Replicate of GrM-14604	—	0.28	74.03 ± 0.19	–22.1	2416 ± 20
Weighted mean: sample x762, T' = 1.1, T' (5%) = 3.8, v = 1, 2431 ± 15 BP								
	KIA-53943	x769	*Quercus* sp. charcoal (Ø > 10 cm) 1 annual ring sampled	—	31.21	73.72 ± 0.23	–23.6	2449 ± 25
	KIA-53944	x774	*Quercus* sp. charcoal (Ø > 10 cm)	—	60.58	73.30 ± 0.22	–25.0	2495 ± 24
Grave A130, urn	KIA-53945	x82 no.1	Charred grass stem	—	68.30	72.49 ± 0.23	–25.1	2585 ± 25
	KIA-53946	x82 no.2	*Triticum* cf. *aestivum*, charred cereal	—	64.19	76.46 ± 0.23	–28.5	2156 ± 24
	KIA-53947	x217	Cremated bone (human)	5.8	0.24	75.57 ± 0.23	–20.9	2250 ± 25
	KIA-53947	X217	Cremated bone (human), replicate	—	—	75.52 ± 0.23	–21.7	2255 ± 25
Weighted mean: sample x217, T' = 0.0, T' (5%) = 3.8, v = 1, 2253 ± 18 BP								
Grave 155, urn	KIA-53948	x127 no.1	cf. *Triticum* sp., charred cereal	—	50.00	73.31 ± 0.22	–26.4	2494 ± 24
	KIA-53949	x127 no.2	*Arrhenatherum elatius* ssp. *Bulbosum*, charred grass bulb	—	65.52	73.56 ± 0.22	–28.2	2466 ± 24
	KIA-53950	x281	Cremated bone (human)	6.1	0.26	74.55 ± 0.23	–23.6	2359 ± 25
	KIA-53950	x281	Cremated bone (human), replicate	—	—	74.41 ± 0.23	–24.1	2374 ± 25

Weighted mean: sample x281, T' = 0.2, T' (5%) = 3.8, v = 1, 2367 ± 18 BP								
Grave A198, urn	KIA-53951	x338	*Alnus* sp. trunk wood charcoal (Ø > 10 cm)	—	57.02	69.12 ± 0.21	–24.9	2967 ± 24
	KIA-53952	x338 CB	Cremated bone (human)	5.9	0.28	74.89 ± 0.24	–24.9	2323 ± 26
	KIA-53952	x338 CB	Cremated bone (human), replicate	—	—	74.82 ± 0.29	–25.9	2330 ± 35
Weighted mean: sample x338 CB, T' = 0.0, T' (5%) = 3.8, v = 1, 2325 ± 21 BP								
Grave A278, urn	KIA-53953	x782 no.1	Charred grass stem	—	74.57	74.17 ± 0.23	–27.5	2400 ± 25
	KIA-53954	x782 no.2	Charred grass, stem and root fragment	—	67.11	73.76 ± 0.23	–26.2	2445 ± 25
	KIA-53955	x783	Cremated bone (human)	5.5	0.2	73.47 ± 0.24	–22.7	2477 ± 26
	KIA-53955	x783	Cremated bone (human), replicate	—	—	73.71 ± 0.23	–22.9	2450 ± 25
Weighted mean: sample x783, T' = 0.6, T' (5%) = 3.8, v = 1, 2463 ± 19 BP								
Grave A393, pit	RICH-25068	x568 no.1	*Triticum dicoccum*, charred cereal	—	61.10	69.69 ± 0.28	–29.9	2901 ± 32
	RICH-25070	x568 no.2	*Hordeum vulgare nudum*, charred cereal	—	44.30	69.58 ± 0.28	–27.2	2914 ± 32
Grave A393, urn	RICH-25341	x561 CB	Cremated bone (human)	6.4	0.16	73.90 ± 0.25	–25.3	2480 ± 27
	KIA-52411	x561 no.1	*Hordeum vulgare nudum*, charred cereal	—	54.67	67.70 ± 0.21	–24.0	3134 ± 25
	KIA-52412	x561 no.3	*Hordeum vulgare nudum*, charred cereal	—	32.35	67.57 ± 0.22	–21.9	3150 ± 27
	KIA-52413	x561 *Quercus*	*Quercus* sp. trunk wood charcoal (Ø > 10 cm)	—	24.78	72.25 ± 0.24	–25.7	2611 ± 27
Grave A394, urn	KIA-52414	x556 no.1	*Alnus* sp. charcoal from branch sapwood (Ø 3-5 cm)	—	26.74	70.77 ± 0.23	–24.9	2778 ± 27
	KIA-53983	X781 no.9	*Acer* sp. trunk wood charcoal (Ø > 10 cm)	—	66.85	68.58 ± 0.21	–27.0	3029 ± 24
	GrM-14708[2]	x785 CB	Cremated bone (human)	6.3	0.10	73.57 ± 0.11	–21.2	2465 ± 18
	KIA-53099[2]	x785 CB	Replicate of GrM-14708	—	0.14	73.97 ± 0.19	–22.7	2422 ± 20
Weighted mean: sample x785 CB, T' = 2.6, T' (5%) = 3.8, v = 1, 2446 ± 14 BP								
	KIA-52415	X785 no.1	*Triticum aestivum*, charred cereal	—	37.76	70.19 ± 0.23	–23.0	2843 ± 26
	KIA-52416	X785 no.4	*Alnus* sp. heartwood charcoal (Ø 2-3 cm)	—	28.07	70.82 ± 0.23	–27.9	2772 ± 26
	KIA-52417	X786 no.1	*Quercus* sp. trunk wood charcoal (Ø > 10 cm)	—	51.01	71.29 ± 0.24	–25.2	2719 ± 27

[2]Two CB samples were replicated between CIO and KIA; they were pretreated in Groningen following the CIO protocol, but were subsequently converted to CO_2 and dated in Kiel (Rose et al. 2019).

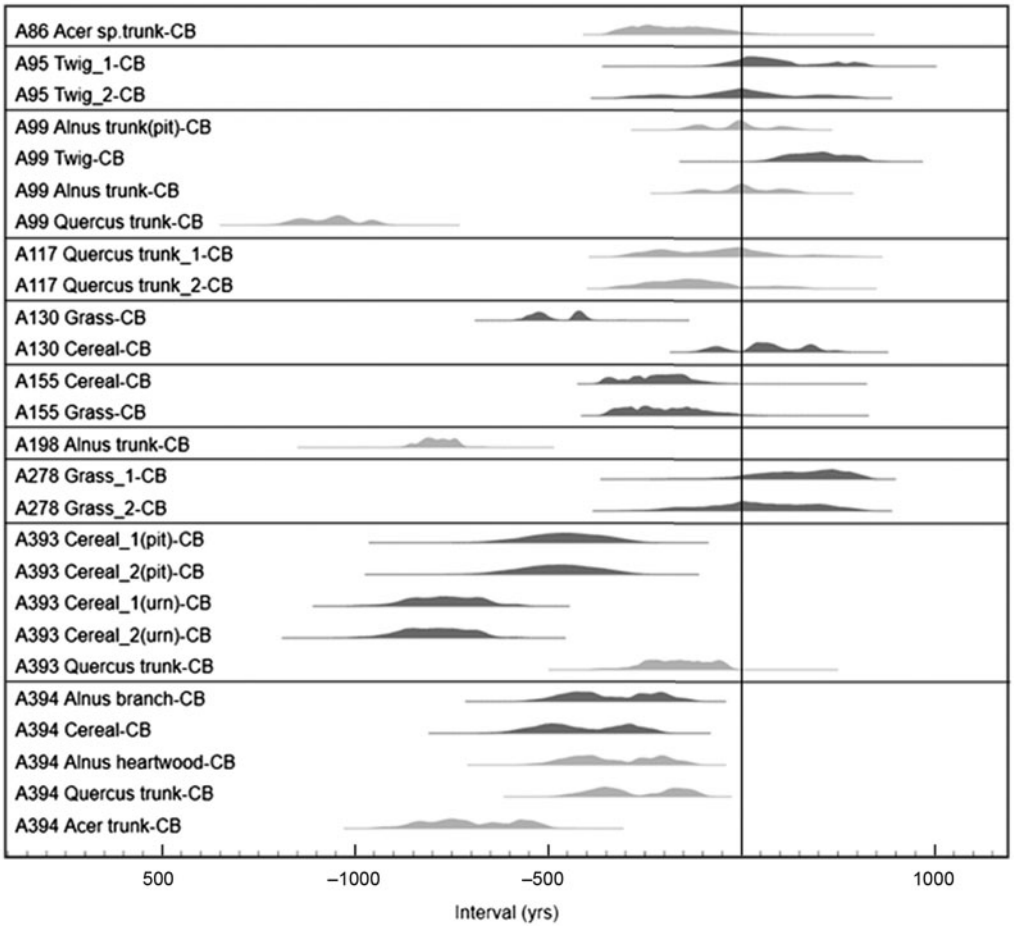

Figure 1 Differences (yr) between calibrated ^{14}C results on context-associated material and CB. Archaeological data set from Aarre urnfield cemetery, grouped by grave. Distributions in black are differences relative to short-lived samples and gray distributions are differences relative to medium- to long-lived samples. Differences that plot on or to the right of the vertical zero line imply that a sample is contemporaneous with or more recent than the CB calibrated date.

All kinds of re-use of an area will severely increase the risk of residual material being re-deposited in a younger context, which appears to have occurred frequently in Aarre. This also underlines the risk of testing the validity of CB dates using associated charcoal dates as "known-age reference material."

Four single cereal grains from the pit and within the urn of grave A393 are considerably older than the associated CB date. Only a single cereal date (KIA-53946, grave A130) is close to its associated CB date. Out of four samples of charred grass, only two (KIA-53953-54) are similar to the associated CB dates or possibly even slightly younger, while the remainder are older. Three dates on charred twigs (KIA-53984-85; RICH-25069) are similar to or younger than their associated CB dates, whereas a date on alder branch sapwood (KIA-52414) is 138–521 yr older (95.4% probability) than the CB. Single entity, short-lived samples from secure, in situ deposits are in general preferred for ^{14}C dating, but as illustrated here the taphonomic processes might be more complicated than otherwise indicated by the archaeological interpretation, and

https://doi.org/10.1017/RDC.2020.3 Published online by Cambridge University Press

samples with negligible IA do not necessarily offer the best estimate of the date of the cremation event.

Experimental Dataset

We report 20 new AMS dates from four separate experimental pyres (Table 4). CI values are generally acceptable (>5), except for pyre no. 16, with three out of four samples having CI values <5, indicating they are not fully calcined. Experiments using archaeological wood proved challenging, as it was difficult to ignite. Pyre no. 9 burned with unusual low, bluish flames omitting an unpleasant sulfurous odor. Even though pyre no. 16 was conducted in the same way as the others, it failed to fully cremate the bone and results from this pyre are not included in the discussion. We suspect the old wood was altered by diagenetic contamination from the burial environment, influencing the pyrotechnical process and complicating the interpretation of ^{14}C measurements. Nevertheless, CB $\delta^{13}C$ (mean = –24.3 ± 2.1 $\delta^{13}C$) and %C (mean = 0.15 ± 0.09 %C) from pyre no. 16 fall within expected ranges and correspond to results observed in archaeological CB (e.g. Olsen et al. 2008). Again, values of $\delta^{13}C$ (measured by AMS) and %C are not directly comparable between laboratories (Rose et al. 2019).

CB ^{14}C ages from individual pyres are statistically inconsistent[1] (Figure 2) (Ward and Wilson 1978). Pyre no. 11 includes both sheep and cattle bone, however, and the combined results on sheep bones are consistent (weighted mean = –442 ± 14 BP), whereas results on cattle bones remain inconsistent, albeit approaching acceptable test values[2]. The maximum difference between ^{14}C ages from individual pyres are highly significant, ranging from 120 ± 28 yr (> 4 σ) to 169 ± 39 yr (> 4 σ). This is an example of how the shape of the ^{14}C calibration curve has an impact on the magnitude of offsets measured in ^{14}C ages. The post-bomb curve is especially steep, thus a small difference in calendar-age offsets between samples will have a large effect on the ^{14}C determinations. The maximum differences between results among sheep or cattle bone samples from pyre no. 11 are smaller but are still significantly different (> 2 σ). These samples come from the same animals, but it is not possible to reconcile the ^{14}C dates from individual experiments without accounting for wood-age offsets in the CB.

Samples from pyres no. 8 and no. 11, using recent wood, have $F^{14}C$ values >1, indicating the presence of bomb ^{14}C (Figure 3a–c), and thus negative ^{14}C ages, whereas samples from pyre no. 9, using medieval wood, have $F^{14}C$ values <1 and positive ^{14}C ages, as a result of mixing carbon reservoirs with different ^{14}C activities (Figure 3d). ^{14}C ages are calibrated in OxCal v4.3 using multiple calibration curves (Bronk Ramsey 2009a). Negative ^{14}C ages are calibrated using the Bomb13NH1 (AD 1650–2010) calibration curve with a 0.5-yr resolution (Hua et al. 2013), with additional data points from the Hammer and Levin datasets (Online Supplementary Information 4) (Levin et al. 2013; Hammer and Levin 2017). Positive ^{14}C ages are calibrated using the IntCal13 Northern Hemisphere atmospheric ^{14}C calibration curve (Reimer et al. 2013).

Carbon exchange results range from 29.3 ± 0.5% to 83.5 ± 0.4% and have an overall mean of 58.6 ± 14.8%. Samples cremated using recent wood have a mean exchange of 52.2 ± 10.9%, ranging from 29.3 ± 0.5% to 67.5 ± 0.5%, whereas experimental pyre no. 9 has a mean exchange of 77.5 ± 5.0%, with a narrower range from 72.3 ± 0.4% to 83.5 ± 0.4%. There appears to be no correlation between % carbon exchange and CI values (Figure 4a), but

[1]Pyre no. 8: T' = 18.4, T'(5%) = 7.8, v = 3. Pyre no. 9: T' = 21.9, T'(5%) = 7.8, v = 3. Pyre no. 11: T' = 30.4, T'(5%) = 14.1, v = 7. Pyre no. 16: T' = 880.5, T'(5%) = 7.8, v = 3.
[2]Pyre no. 11 cattle: T' = 9.0, T'(5%) = 7.8, v = 3, sheep: T' = 7.6, T'(5%) = 7.8, v = 3.

https://doi.org/10.1017/RDC.2020.3 Published online by Cambridge University Press

Table 4 Radiocarbon results on the experimental data set.

Context	Cremation duration (hr)	Lab code	Sample ID	Material	CI	%C	$F^{14}C$	Corrected pMC	AMS $\delta^{13}C$ (‰VPDB)[1]	Conventional ^{14}C age (BP)	% C exchange with old CO_2 $F^{14}C$ indicated
Pyre no. 8	2	RICH-25820	x231_1	Cremated bone (*Ovis aries*)	6.6	0.39	1.0443 ± 0.0018	104.43 ± 0.31	–21.4	–348 ± 24	29.3 ± 0.5
		RICH-25821	x231_2	Cremated bone (*Ovis aries*)	6.2	0.16	1.0632 ± 0.0031	106.32 ± 0.31	–26.0	–492 ± 24	55.5 ± 0.5
		RICH-25822	x231_3	Cremated bone (*Ovis aries*)	5.6	0.20	1.0559 ± 0.0033	105.59 ± 0.33	–24.8	–437 ± 25	45.4 ± 0.5
		RICH-25823	x231_4	Cremated bone (*Ovis aries*)	5.9	0.12	1.0543 ± 0.0038	105.43 ± 0.38	–21.2	–425 ± 29	43.2 ± 0.5
Pyre no. 9	2.5	GrM-14698	x238_1	Cremated bone (*Bos taurus*)	5.7	0.12	0.9332 ± 0.0023	93.32 ± 0.23	–22.1	555 ± 20	72.3 ± 0.4
		GrM-14700	x238_2	Cremated bone (*Bos taurus*)	7.0	0.10	0.9242 ± 0.0023	92.42 ± 0.23	–22.6	635 ± 20	79.5 ± 0.4
		GrM-14701	x238_3	Cremated bone (*Bos taurus*)	5.5	0.08	0.9303 ± 0.0024	93.03 ± 0.24	–22.9	580 ± 20	74.6 ± 0.4
		GrM-14702	x238_4	Cremated bone (*Bos taurus*)	5.6	0.10	0.9192 ± 0.0023	91.92 ± 0.23	–25.3	675 ± 20	83.5 ± 0.4
Pyre no. 11	2	RICH-25737	x246_1	Cremated bone (*Bos taurus*)	6.0	0.07	1.0719 ± 0.0039	107.19 ± 0.39	–25.4	–558 ± 29	67.5 ± 0.5
		RICH-25738	x246_2	Cremated bone (*Bos taurus*)	6.7	0.06	1.0714 ± 0.0039	107.14 ± 0.39	–27.1	–554 ± 29	66.8 ± 0.5
		RICH-25739	x246_3	Cremated bone (*Bos taurus*)	6.8	0.34	1.0587 ± 0.0034	105.87 ± 0.34	–22.9	–458 ± 26	49.2 ± 0.5
		RICH-25740	x246_4	Cremated bone (*Bos taurus*)	6.6	0.21	1.0648 ± 0.0034	106.48 ± 0.34	–23.9	–504 ± 26	57.7 ± 0.5
		RICH-25744	x246_5	Cremated bone (*Ovis aries*)	6.2	0.12	1.0629 ± 0.0038	106.29 ± 0.38	–27.1	–490 ± 29	60.4 ± 0.5
		RICH-25745	x246_6	Cremated bone (*Ovis aries*)	6.1	0.14	1.0496 ± 0.0033	104.96 ± 0.33	–23.6	–389 ± 26	44.2 ± 0.5
		RICH-25753	x246_7	Cremated bone (*Ovis aries*)	8.5	0.16	1.0594 ± 0.0035	105.94 ± 0.35	–28.5	–464 ± 27	56.2 ± 0.5
		RICH-25754	x246_8	Cremated bone (*Ovis aries*)	6.8	0.10	1.0556 ± 0.0039	105.56 ± 0.39	–24.0	–434 ± 30	51.5 ± 0.5
Pyre no. 16	2	GrM-14692	x251_1	Cremated bone (*Ovis aries*)	4.3	0.24	0.9467 ± 0.0024	94.67 ± 0.24	–26.8	440 ± 20	—
		GrM-14693	x251_2	Cremated bone (*Ovis aries*)	5.5	0.23	0.9366 ± 0.0023	93.66 ± 0.23	–31.3	525 ± 20	—
		GrM-14695	x251_3	Cremated bone (*Ovis aries*)	4.6	0.11	0.8791 ± 0.0022	87.91 ± 0.22	–30.5	1035 ± 20	—
		GrM-14697	x251_4	Cremated bone (*Ovis aries*)	4.1	0.14	0.9703 ± 0.0024	97.03 ± 0.24	–22.3	240 ± 20	—

[1]Measured by AMS. Values are not the true ^{13}C values of the investigated materials, as they are affected by isotope fractionation during acid extraction, graphitization and AMS measurement.

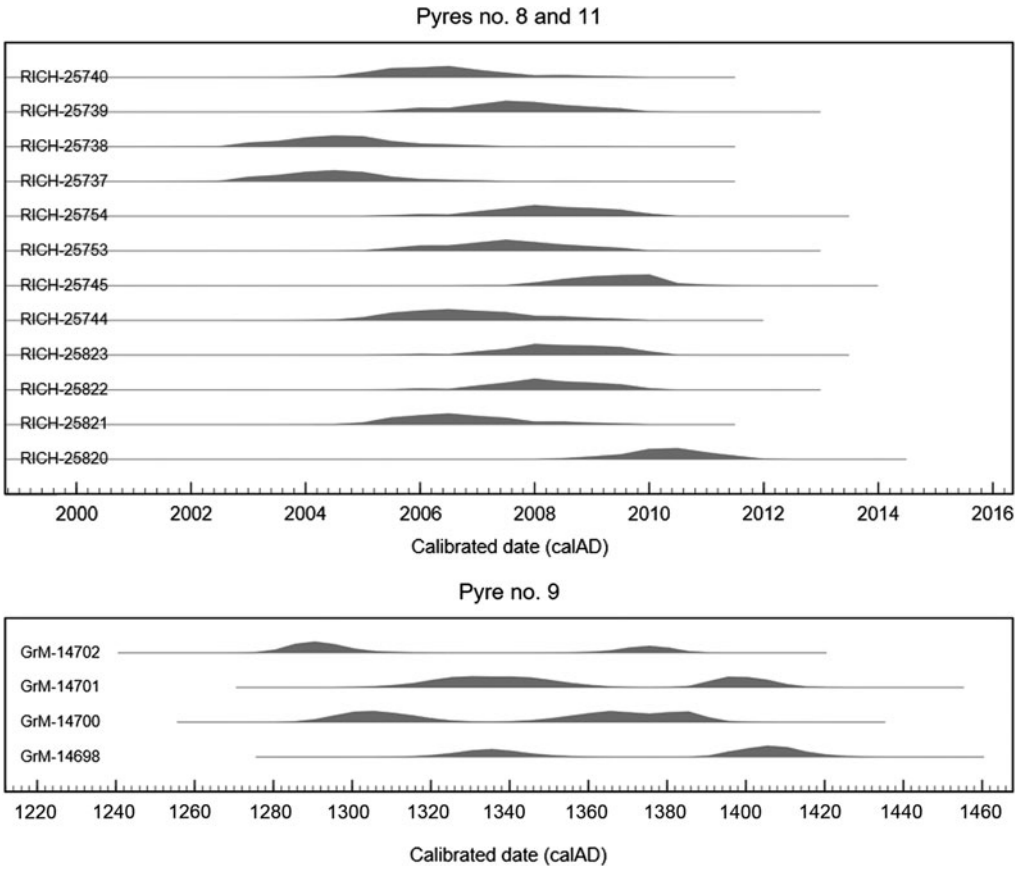

Figure 2 Calibrated ^{14}C results on the experimental data set. Results from pyre no. 9 are calibrated using the IntCal13 Northern Hemisphere atmospheric ^{14}C data set (Reimer et al. 2013). Results from pyres no. 8 and 11 are calibrated using the Bomb13NH1 (AD1650–2010) calibration curve (Hua et al. 2013) with additional data points from the Hammer and Levin datasets of atmospheric ^{14}C activity from Jungfraujoch in the Swiss Alps (Levin et al. 2013; Hammer and Levin 2017).

there is a clear relationship between % carbon exchange and duration of the cremations (hr) (Figure 4b). Pyre no. 9 was burning for ca. 30 min longer than the others and produced higher carbon exchange percentages, but it is difficult to ascertain whether this apparent difference in range is caused by the longer cremation duration itself or by possible differences in temperatures (not measured) and type of fuel wood. The bone apatite, bone collagen and wood from pyres no. 8 and no. 11 have similar ages, and we cannot rule out collagen might have contributed to the carbon composition of the pyre atmosphere. This could possibly explain the smaller % carbon exchange, as compared to pyre no. 9. Values of % carbon exchange and $\delta^{13}C$ appear to be related, but do not suggest a clear linear mixing model between unburned apatite and wood (Figure 4c).

DISCUSSION

We have presented results from 10 archaeological graves with a combination of ^{14}C dated CB and associated material. Charcoal samples from oak trunk wood can have considerable IA, and even trunk wood samples of shorter-lived alder and maple have an average ^{14}C signal

https://doi.org/10.1017/RDC.2020.3 Published online by Cambridge University Press

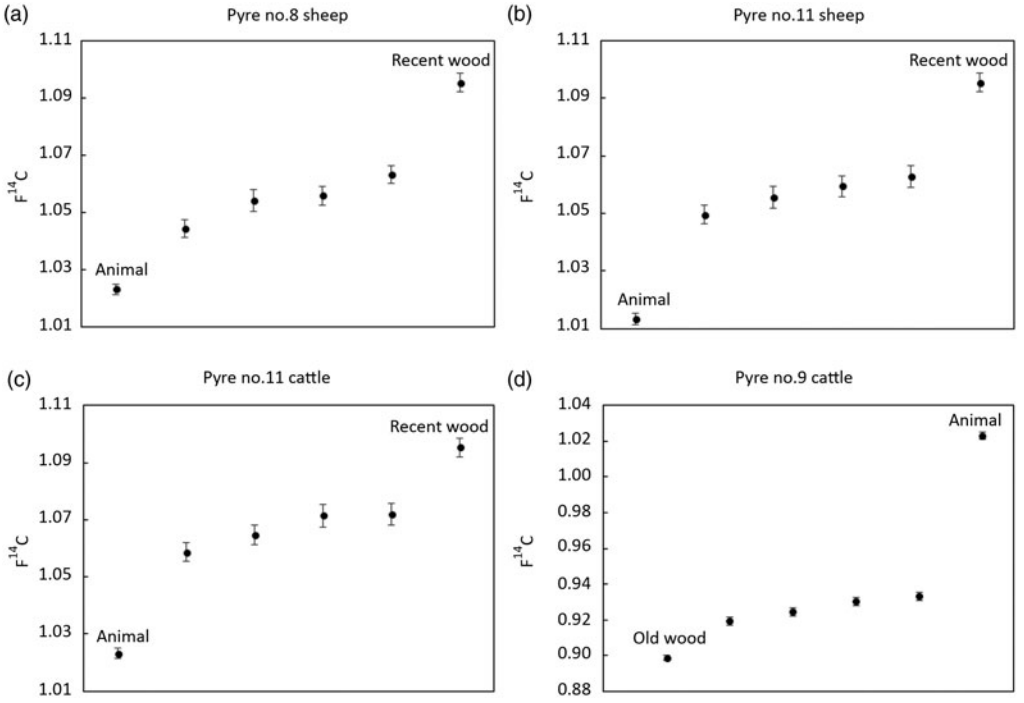

Figure 3 Experimental $F^{14}C$ results with 1σ uncertainties: (a) pyre no. 8 sheep, (b) pyre no. 11 sheep, (c) pyre no. 11 cattle and (d) pyre no. 9 cattle. Endmember values of animal and wood indicated directly in the figures.

predating the cremation event and can, with a high % carbon exchange, cause a significant wood-age offset in the CB. Two charcoal samples of alder trunk wood from grave A99 have calibrated dates agreeing with the CB date, whereas a charred twig dates younger. A charcoal sample of oak trunk wood from the same grave predating the other samples by approximately a millennium is probably residual and unrelated to the grave. In this scenario the twig with negligible IA will best reflect the date of the cremation event. In the following, we will focus on graves containing short-lived samples (i.e. with negligible IA). Furthermore, because wood-age offsets can only make the CB older (unless old bone is cremated with young wood, which is an unlikely archaeological scenario), we ignore short-lived samples dating older than the CB, and only discuss samples whose dates are similar to or later than the date of the associated CB (i.e. differences plot on or to the right of the zero line in Figure 1). We regard the calibrated dates of these short-lived samples as dating the cremation event, and thus indicating possible wood-age offsets in the CB samples.

Graves A95, A99, A130 and A278 contain material meeting these criteria. Graves A95 and A278 each provided two such short-lived samples with statistically consistent ^{14}C ages, whose weighted means (A95: 2399 ± 19 BP, df = 1, T' = 2.8 (5% = 3.8); A278: 2423 ± 18 BP, df = 1, T' = 1.6 (5% = 3.8)) provide better estimates of the dates of the respective cremations. The calibrated date differences between CB and short-lived samples are assumed to be exponentially distributed and modeled in a bounded phase starting at zero and ending with a Tau_Boundary (Bronk Ramsey 2009a). Results are summarized in a KDE_Plot in Figure 5 (Bronk Ramsey 2017). The posterior distribution estimate differences to have a median of 62 yr and a 1-σ range of 173 yr (Online Supplementary Information 1, Part 2). The median offset is larger than we

https://doi.org/10.1017/RDC.2020.3 Published online by Cambridge University Press

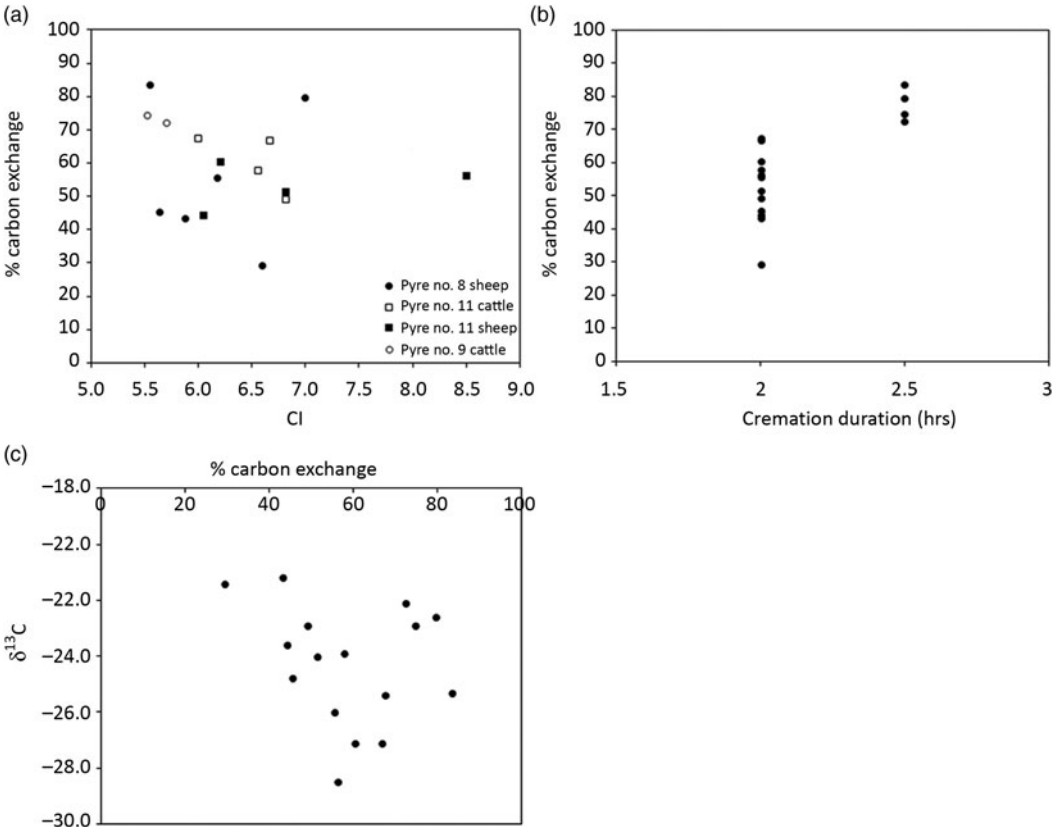

Figure 4 Results of % carbon exchange plotted against different measurement parameters of the experimental data set: (a) % carbon exchange plotted against CI, (b) % carbon exchange plotted against cremation duration (hr) and (c) % carbon exchange plotted against $\delta^{13}C$ values.

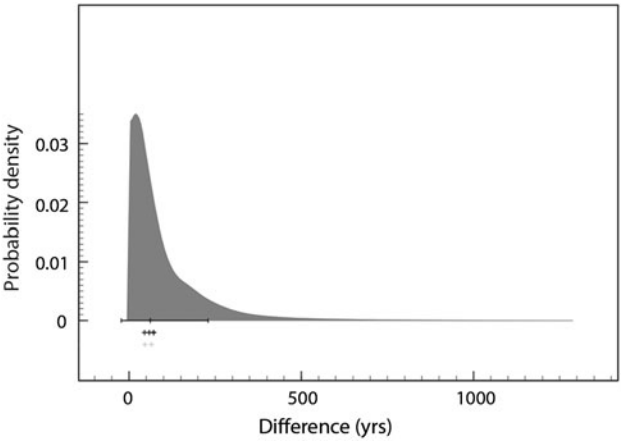

Figure 5 Constrained differences between selected short-lived samples and CB (see text) summarized in a KDE_Plot. Differences calculated using weighted means of short-lived samples from grave A95 (2399 ± 19 ^{14}C yr, df = 1, T' = 2.8 (5% = 3.8) and grave A278 (2423 ± 18 ^{14}C yr, df = 1, T' = 1.6 (5% = 3.8)). Median offset of 62 yr and a 1-σ range of 173 yr. Black bar indicates the 1σ range and crosses the median values of individual differences.

https://doi.org/10.1017/RDC.2020.3 Published online by Cambridge University Press

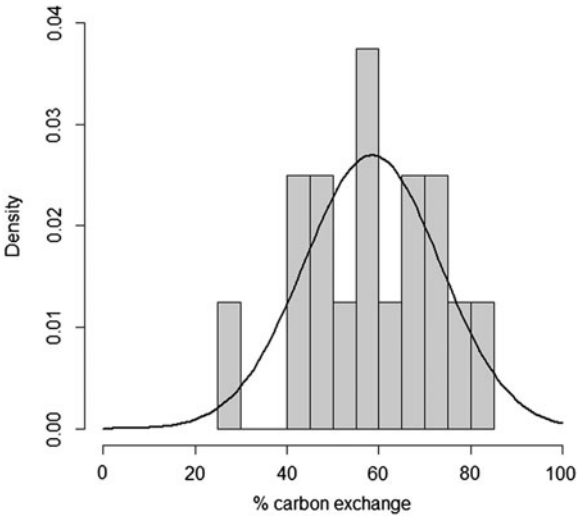

Figure 6 Density plot of % carbon exchange from the experimental data set (gray bars). The added curve depicts 1000 random numbers drawn from a normal distribution with mean and standard deviation derived from the experimental data set.

have just modeled for combined legacy dates from Bronze Age Denmark and medieval Japan (median = 22 yr, 1-σ range = 32 yr), although they do overlap within 1-σ ranges (Olsen et al. 2008; Olsen et al. 2013; Minami et al. 2019). The median of the archaeological differences falls within the 50–100 yr offset that has been suggested in the literature, although this now looks to underestimate the total range (Hüls et al. 2010; Van Strydonck et al. 2010; Zazzo and Saliège 2011; Snoeck et al. 2014).

Experimental cremation studies have documented a high degree of carbon substitution both in laboratory and open-air experimental setups (Hüls et al. 2010; Van Strydonck et al. 2010; Zazzo et al. 2012; Snoeck et al. 2014). Our open-air experimental results show similarly wide substitution ranges in samples from the same individual (animal cut) when the pyre is fueled by recent wood (pyre no. 8 and no. 11: from 29.3 ± 0.5% to 67.5 ± 0.5% with mean exchange 52.2 ± 10.9%), whereas using old wood (pyre no. 9: from 72.3 ± 0.4% to 83.5 ± 0.4% with mean exchange 77.5 ± 5.0%) produce slightly more consistent results. The variability in CB $F^{14}C$ within each pyre is exaggerated due to large differences in ^{14}C content of the old wood and modern bone amplifying the effect of % carbon exchange differences between bone fragments, and perhaps due to the ^{14}C inhomogeneity of the recent wood affected by the ^{14}C bomb spike. We would therefore expect less variation in CB ^{14}C ages from real prehistoric cremations. Figure 3b indicates a possible correlation of % carbon exchange and cremation duration, which requires further investigation. However, a density plot of % carbon exchange (Figure 6) closely resembles a normal distribution, suggesting that the expected wood-age offsets in CB within individual pyres will be normally distributed.

The only source of carbon in bio-apatite is carbonate ions formed through energy production in cells, which can substitute with hydroxyl (OH, A-type carbonates) or phosphate (PO_4, B-type

https://doi.org/10.1017/RDC.2020.3 Published online by Cambridge University Press

carbonates) in the bone-matrix (Lee-Thorp 2008; Hüls et al. 2010). This results in an IA of the bio-apatite equal to the turn-over rate of the bone-matrix, probably comparable to turn-over rates in bone-collagen (Hedges et al. 2007). This leads us to expect IA of the carbon in the original bio-apatite to be unevenly distributed throughout a human skeleton, but given the short lifespan of the animals used in our experiments, their ^{14}C contents must be fairly homogenous. Thus, the large dispersion of % carbon exchange results in CB from a single pyre must here reflect a differential uptake of exogenous carbon, but also variations in temperature and CO_2 concentration within a small pyre might play a role. Our % carbon exchange results underline a certain degree of dispersion is to be expected when ^{14}C dating CB, which again points to the need of handling these offsets statistically.

Outlier Modeling

We consider the calibrated offsets between CB and selected short-lived samples from the archaeological data set, and find the distribution in Figure 5 to visually resemble the exponentially distribution otherwise expected for charcoal dates, i.e. most samples dating close to the event in question, but a diminishing number of samples dating increasingly older (Nicholls and Jones 2001; Dee and Bronk Ramsey 2014). OxCal's default Charcoal OM may therefore be a reasonable model for dealing with wood-age offsets in CB, as proposed by Garrow et al. (2014) and Fitzpatrick et al. (2017). All modeling is conducted in OxCal v4.3 (Bronk Ramsey 2009a, 2009b).

To test this idea, we model the archaeological results from Aarre urnfield cemetery as a bounded phase of activity. Individual graves are modeled as phases including dates on CB and selected short-lived samples, except graves A95, A99, A130 and A278 where CB dates are combined with dates on contemporaneous, short-lived samples. Dates of charcoal samples with potentially significant IA are modeled as *terminus post quem* (TPQ) dates. In *Model 1* (Online Supplementary Information 1, Part 3, Model 1), we apply the Charcoal OM to all CB dates, with a prior probability of 1 (i.e. all CB dates are assumed to be affected by wood-age offsets). The Charcoal OM posterior estimates the CB dates to date 2–91 yr or 0–252 yr older than their cremation events (68.2% and 95.4% probabilities), with a median of 55 yr. The offsets agree within the 68.2% probability range with the offsets otherwise indicated by the calibrated differences between selected short-lived material and CB (median 62 yr and 1-σ range 173 yr), although the Charcoal OM might underestimate the offsets slightly.

Based on our experimental results, the CB dates should always fall between the short-lived sample dates and the average age of charcoal, although individual fragments of charcoal can be younger than the CB. The pyre wood will have an IA some years older than the cremation event, as will carbon in the unburned bio-apatite. Both are type-t offsets (on the calendar scale, as opposed to "type-r" offsets in ^{14}C space, such as dietary reservoir effects). In *Model 2* (Figure 7a) we apply a minimum offset to all CB dates, by creating a "Cremation OM" (Online Supplementary Information 1, Part 3, Model 2). This uses the same exponential distribution as the default Charcoal OM, but with an exponential constant of 0.9 and running from –10 to –0.1 to ensure the peak of the OM posterior distribution is shifted away from zero. The scale parameter is set to U(1,3), rather than U(0,3), i.e. offsets can vary between 10^1 and 10^3 rather than 10^0–10^3 yr, reducing the chances of sub-decadal offsets. We apply the Cremation OM to all CB dates, with a prior probability of 1, and otherwise construct *Model 2* as *Model 1*. The Cremation OM

https://doi.org/10.1017/RDC.2020.3 Published online by Cambridge University Press

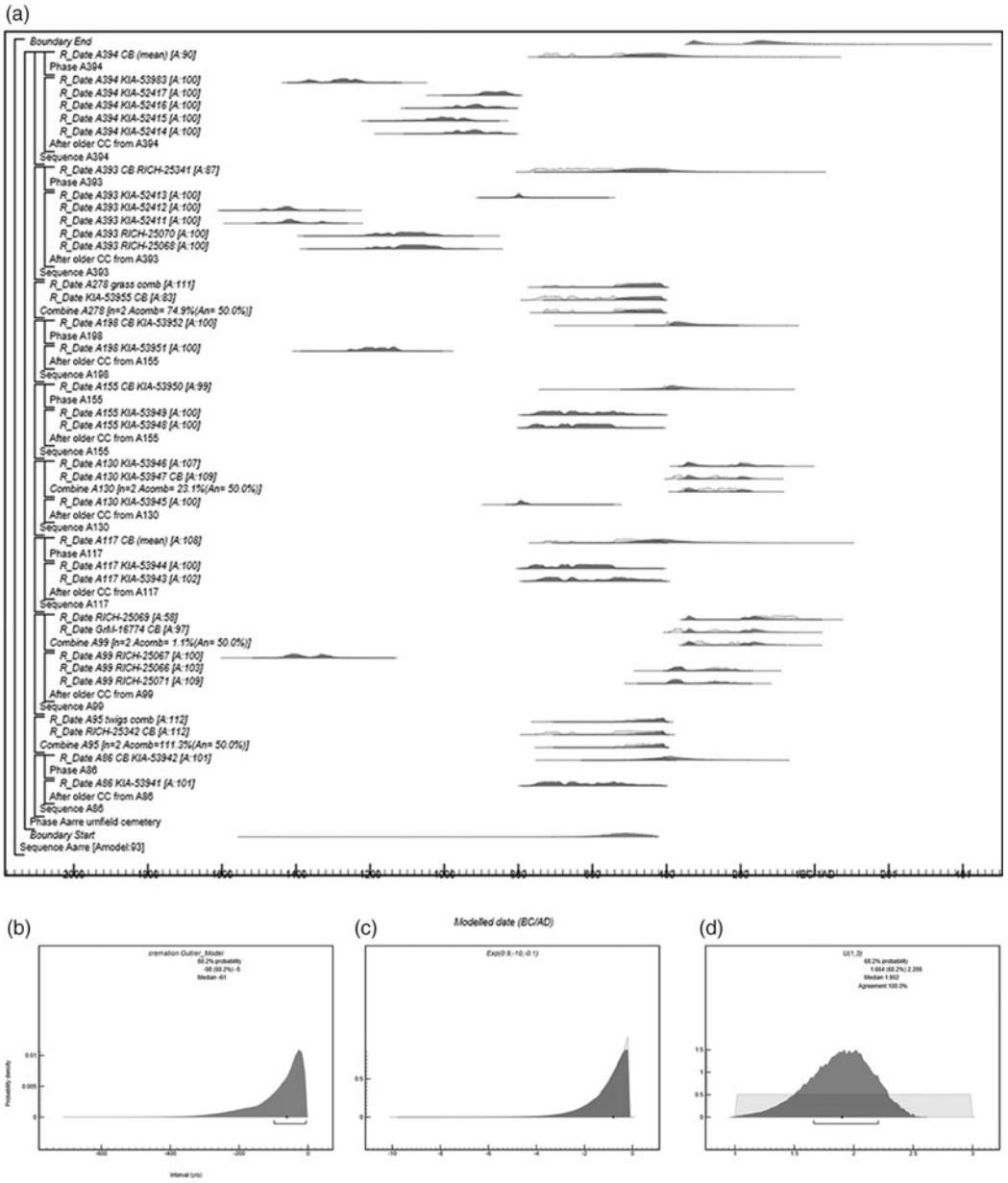

Figure 7 Chronological *Model 2* of all ^{14}C results from Aarre urnfield cemetery (a) with a bespoke cremation outlier model applied to CB dates. In the middle left plot (b) is the posterior distribution of the outlier offsets (5–98 yr with 68% probability). In the middle right plot (c) is the effective prior and in the lower plot (d) the estimated timescale for wood-age offset in CB (posterior distribution in gray and uniform prior shown in outline).

estimates the CB dates to date 5–98 yr or 2–252 yr older than their cremation events (68.2% and 95.4% probabilities), with a median of 61 yr (Figure 7b–d). The Cremation OM estimates larger offsets than the Charcoal OM does, and the offset median is very close to the median suggested by our archaeological material.

https://doi.org/10.1017/RDC.2020.3 Published online by Cambridge University Press

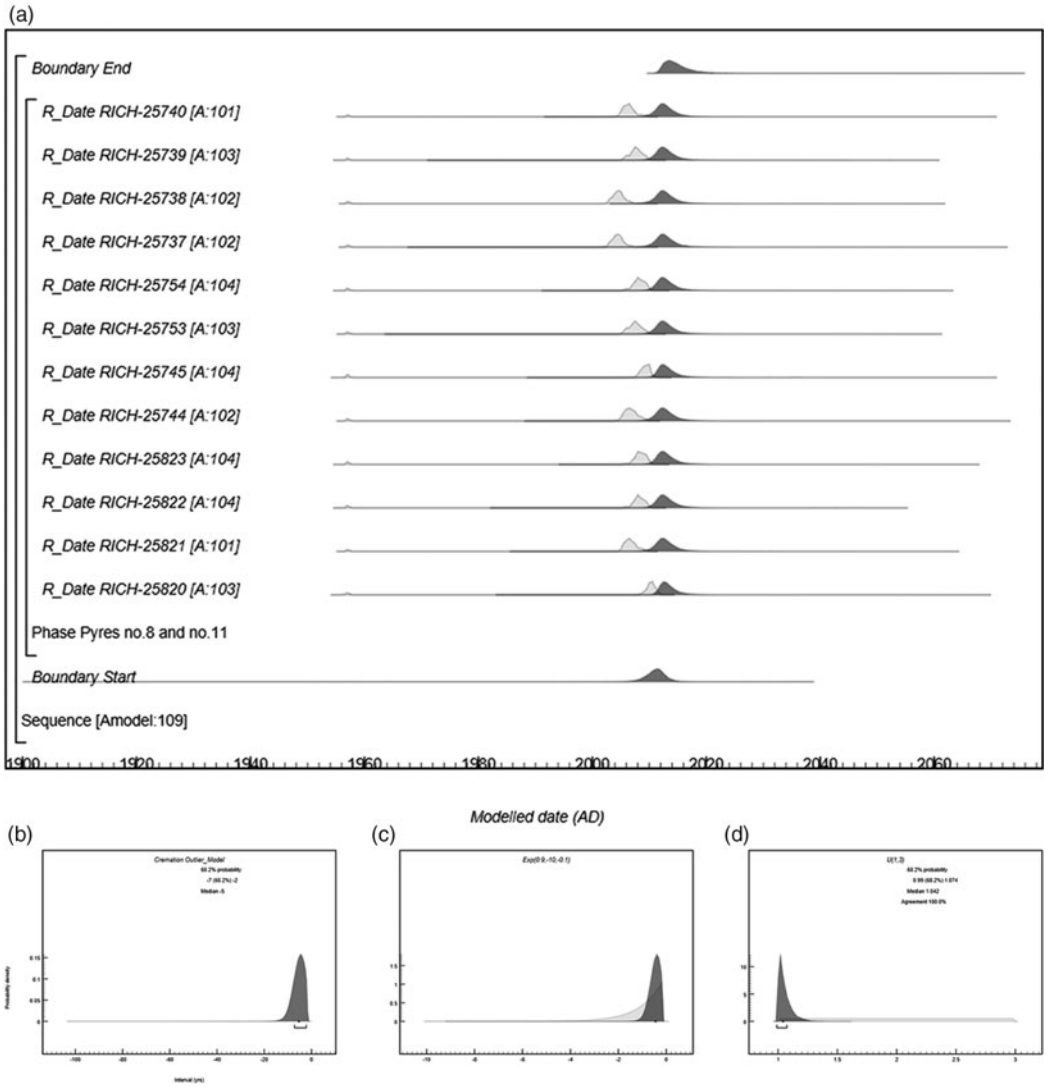

Figure 8 Chronological *Model 4* applying a Cremation OM to experimentally CB (a). In the middle left plot (b) is the posterior distribution of the outlier offsets (2–7 yr with 68.2% probability). In the middle right plot (c) is the effective prior and in the lower plot (d) the estimated timescale for wood-age offset in CB (posterior distribution in gray and uniform prior shown in outline).

Next we test the suitability of both Charcoal and Cremation OM for estimating wood-age offsets in our experimental data set using recent wood (pyres no. 8 and no. 11). In *Model 3* (Online Supplementary Information 1, Part 4, Model 3), we treat the CB dates as representing a bounded phase of activity and apply a Charcoal OM to the CB dates with a probability of 1. The model estimates activity to start AD 2004–2010 and end AD 2008–2012 (95.4% probability, $A_{model} = 96$) and the posterior distribution of the OM estimate the CB dates to date 0–2 yr or 0–5 yr older than their cremation events (68.2% and 95.4% probabilities). *Model 3* estimates the cremation events to have occurred before the actual event (AD 2013 and 2015), meaning that the Charcoal OM underestimate the wood-age offsets.

https://doi.org/10.1017/RDC.2020.3 Published online by Cambridge University Press

Given the short lifespans of the experimental material it will have a shorter residence time of the unburned bio-apatite, compared to the human CB from the archaeological material. The IA of the pyre wood will however still cause a minimum wood-age offset, why we create *Model 4* with the same chronological construction as described above. We apply the bespoke Cremation OM to the CB dates, with a prior probability of 1 (Figure 8a, Online Supplementary Information 1, Part 4, Model 4). The OM takes all adjusted parameters as described for *Model 2*. *Model 4* ($A_{model} = 109$) estimates activity to start AD 2006–2014 and end AD 2011–2021 (95.4% probability). The posterior distribution of the Cremation OM estimates the CB dates to date 2–7 yr or 1–11 yr older than their cremation events (68.2% and 95.4% probabilities, Figure 8b–d). These offsets are larger than calculated by the Charcoal OM and enable *Model 4* to estimate start and end boundaries encompassing the true dates of the cremation events.

It is difficult to assess which OM model is best suited for the archaeological data set, as we do not know the true cremation dates. But we find it to be a convincing argument, that the Cremation OM yields a median offset similar to that suggested by differences between the calibrated dates of short-lived material and associated CB. For the experimental data set, the Charcoal OM underestimates the observed offsets, whereas the Cremation OM enables the chronological model to accurately date the cremation events. Earlier studies (Garrow et al. 2014; Fitzpatrick et al. 2017) have used outlier modeling to handle wood-age offsets in CB, but with new empirical data on the scale and distribution of these offsets we can suggest a bespoke Cremation OM with a minimum offset to be better suited to our purposes than the default Charcoal OM.

CONCLUSION AND IMPLICATIONS FOR ARCHAEOLOGY

We have demonstrated significant variation in carbon exchange in experimentally CB, with % carbon exchange among samples from single pyres ranging from $29.3 \pm 0.5\%$ to $83.5 \pm 0.4\%$ (mean $58.6 \pm 14.8\%$). We have confirmed that wood-age offsets in archaeological CB are significant, with a 62 yr median calibrated date offset between short-lived, context associated material and CB (1-σ range of 173 yr). The distribution of wood-age offsets appears to follow an exponential distribution and we test if the default Charcoal OM is applicable for estimating such offsets in archaeological and experimental CB but find that it slightly underestimates apparent offsets. To counter the intrinsic age of both pyre fuel and unburned bio-apatite we instead propose a bespoke Cremation OM, which combines an exponential distribution of calendar age offsets with a minimum offset, and provides better estimates of the actual dates of cremations.

It is important to stress that carbon exchange can vary even within a single cremated bone, and that the shape of the ^{14}C calibration curve can have great impact on the magnitude of these offsets measured in ^{14}C age. Instead of trying to quantify and correct for the offset individually, we urge that they be treated statistically using formal outlier modeling.

ACKNOWLEDGMENTS

Analyses were funded through the Center for Baltic and Scandinavian Archaeology (ZBSA)'s Man and Environment research theme and by the Deutsche Forschungsgemeinschaft (DFG, German Research Foundation – Project number 2901391021 – SFB 1266) subproject G1: Timescales of Change – Chronology of cultural and environmental transformations of the Collaborative Research Center "Scales of Transformation: Human-environmental

Interaction in Prehistoric and Archaic Societies". The authors would like to thank Odense City Museums and ARKVEST – Arkæologi Vestjylland for access to material. We are thankful to Ingeborg Levin and Samuel Hammer from the Institute of Environmental Physics at Heidelberg University for letting us work with their recent measurements of atmospheric ^{14}C activity from Jungfraujoch in the Swiss Alps. Without this it would not have been possible to analyze our post-bomb data.

SUPPLEMENTARY MATERIAL

To view supplementary material for this article, please visit https://doi.org/10.1017/RDC.2020.3

REFERENCES

Bayliss A. 1999. On the taphonomy of charcoal samples for radiocarbon dating. In: Evin J, editor. Actes du 3ème Congrès International 14 C et Archéologie: Lyon 6-10 avril 1998. Paris: Soc. Préhist. Française. p 51–6.

Becker CJ. 1961. Førromersk jernalder i Syd- og Midtjylland. Kbh.: Nationalmuseet.

Boudin M, Van Strydonck M, van den Brande T, Synal H-A, Wacker L. 2015. RICH – A new AMS facility at the Royal Institute for Cultural Heritage, Brussels, Belgium. Nuclear Instruments and Methods in Physics Research Section B: Beam Interactions with Materials and Atoms 361:120–3.

Bronk Ramsey C. 2009a. Bayesian analysis of radiocarbon dates. Radiocarbon 51(1):337–60.

Bronk Ramsey C. 2009b. Dealing with outliers and offsets in radiocarbon dating. Radiocarbon 51(3):1023–45.

Bronk Ramsey C. 2017. Methods for summarizing radiocarbon datasets. Radiocarbon:1–25.

Chatters JC, Brown JW, Hackenberger S, McCutcheon P, Adler J. 2017. Calcined bone as a reliable medium for radiocarbon dating: A test using paired North American samples. American Antiquity 82(3):593–608.

Daly A. 2011. Dendrochronological analysis of timbers from a well at Odense Adelige Jomfrukloster, Fyn. OBM137 Dendro.dk.

Daly A. 2014. Dendrochronological analysis of timbers from a well at Skovgård, Sdr. Nærå, Fyn. OBM 1613. Dendro.dk.

De Mulder G, Van Strydonck M, Boudin M. 2009. The impact of cremated bone dating on the archaeological chronology of the Low Countries. Radiocarbon 51(2):579–600.

Dee MW, Bronk Ramsey C. 2014. High-precision Bayesian modeling of samples susceptible to inbuilt age. Radiocarbon 56(1):83–94.

Dee MW, Palstra SWL, Aerts-Bijma AT, Bleeker MO, de Bruijn S, Ghebru F, Jansen HG, Kuitems M, Paul D, Richie RR, Spriensma JJ, Scifo A, van Zonneveld D, Verstappen-Dumoulin BMAA, Wietzes-Land P, Meijer HAJ. 2019. Radiocarbon dating at Groningen: New and updated chemical pretreatment procedures. Radiocarbon:1–12.

Effenberger H. 2017a. Report about the results of the charcoal analysis and selection of datable material for the sites HOM and VAM1600. Effenberger Archäobotanik.

Effenberger H. 2017b. Report about the results of the charcoal analysis and selection of datable material for the sites ARV113 and VAM1600. Effenberger Archäobotanik.

Effenberger H. 2019. Report about the results of the charcoal analysis and selection of datable material for the site VAM1600. Effenberger Archäobotanik.

Fitzpatrick AP, Hamilton WD, Haselgrove CC. 2017. Radiocarbon dating and Bayesian modelling of the Late Iron Age cremation burial cemetery at Westhampnett, West Sussex, GB. Archaeologisches Korrespondenzblatt 47:359–81.

Garrow D, Meadows J, Evans C, Tabor J. 2014. Dating the dead: A high-resolution radiocarbon chronology of burial within an Early Bronze age barrow cemetery at Over, Cambridgeshire. Proceedings of the Prehistoric Society 80:207–36.

Grootes PM, Nadeau M-J, Rieck A. 2004. ^{14}C-AMS at the Leibniz-Labor: Radiometric dating and isotope research. Nuclear Instruments and Methods in Physics Research Section B: Beam Interactions with Materials and Atoms 223–224:55–61.

Hammer S, Levin I. 2017. Monthly mean atmospheric $D^{14}CO_2$ at Jungfraujoch and Schauinsland from 1986 to 2016. heiDATA Dataverse.

Hedges REM, Clement JG, Thomas CDL, O'Connell TC. 2007. Collagen turnover in the adult femoral mid-shaft: Modeled from anthropogenic radiocarbon tracer measurements. American Journal of Physical Anthropology 133(2):808–16.

Henriksen MB. 2009. Brudager Mark – en romertidsgravplads nær Gudme på Sydøst Fyn.

Henriksen MB. 2016. Bålets betydning [Doctoral dissertation]: Copenhagen University.

Henriksen MB. 2019. Experimental cremations – can they help us to understand prehistoric cremation graves? In: Cieśliński A, Kontny B, editors. Interacting barbarians contacts, exchange and migrations in the first millennium AD. Warschau: Neue Studien zur Sachsenforschung Band 9. p 289–96.

Hissel M, Parlevliet M, Verspay J. 2007. Begraven, bewonen, beakkeren. Archeologisch onderzoek bij de uitbreiding van de woonwijk Genoenhuis, gemeente Geldrop-Mierlo (Noord-Brabant). Amsterdam.

Hornstrup KM, Glintborg Overgaard K, Andersen S, Bennike P, Hambro Mikkelsen P, Malmros C. 2005. Hellegård – en gravplads fra omkring år 500 f. Kr. Aarbøger for Nordisk Oldkyndighed og Historie 2002:83–162.

Hua Q, Barbetti M, Rakowski AZ. 2013. Atmospheric Radiocarbon for the Period 1950–2010. Radiocarbon 55(04):2059–72.

Hüls CM, Erlenkeuser H, Nadeau MJ, Grootes PM, Andersen N. 2010. Experimental study on the origin of cremated bone apatite carbon. Radiocarbon 52(2):587–99.

Iversen J. 1974. The development of Denmark's nature since the Last Glacial.

Jensen CK. 1996. Chronologische Probleme der Vorrömische Eisenzeit Dänemarks. Praehistorische Zeitschrift 1996(2):194–216.

Lanting JN, Aerts-Bijma AT, van der Plicht J. 2001. Dating of cremated bones. Radiocarbon 43(2A):249–54.

Lee-Thorp JA. 2008. On isotopes and old bones. Archaeometry 50(6):925–50.

Levin I, Kromer B, Hammer S. 2013. Atmospheric $\Delta^{14}CO_2$ trend in Western European background air from 2000 to 2012. Tellus B: Chemical and Physical Meteorology 65(1):20092.

Lorange T. 2015. Det sakrale landskab ved Årre. Landskabets hukommelse gennem 4.000 års gravriter. In: Foss P, Møller NA, editors. De dødes landskab. Grav og gravskik i ældre jernalder i Danmark. Ribe: SAXO-instituttet, Københavns Universitet. p 21–36.

Martín-Seijo M, César Vila M. 2018. Oak, ash and pine: The role of firewood in funerary rituals at the Roman site of Reza Vella (Ourense, Spain). Archaeological and Anthropological Sciences.

Minami M, Mukumoto H, Wakaki S, Nakamura T. 2019. Effect of crystallinity of apatite in cremated bone on carbon exchanges during burial and reliability of radiocarbon dating. Radiocarbon:1–12.

Moskal-del Hoyo M. 2012. The use of wood in funerary pyres: Random gathering or special selection of species? Case study of three necropolises from Poland. Journal of Archaeological Science 39(11): 3386–95.

Nadeau MJ, Grootes PM, Schleicher M, Hasselberg P, Rieck A, Bitterling M. 1997. Sample throughput and data quality at the Leibniz-Labor AMS Facility. Radiocarbon 40(1):239–45.

Naysmith P, Scott EM, Cook GT, Heinemeier J, Van der Plicht J, Van Strydonck M, Bronk Ramsey C, Grootes PM, Freeman SPHT. 2007. A cremated bone intercomparison study. Radiocarbon 49(2):403–8.

Nicholls G, Jones M. 2001. Radiocarbon dating with temporal order constraints. Journal of the Royal Statistical Society. Series C (Applied Statistics) 50(4):503–21.

O'Donnell L. 2016. The power of the pyre – A holistic study of cremation focusing on charcoal remains. Journal of Archaeological Science 65:161–71.

Olsen J, Heinemeier J, Bennike P, Krause C, Margrethe Hornstrup K, Thrane H. 2008. Characterisation and blind testing of radiocarbon dating of cremated bone. Journal of Archaeological Science 35(3):791–800.

Olsen J, Heinemeier J, Hornstrup KM, Bennike P, Thrane H. 2013. 'Old wood' effect in radiocarbon dating of prehistoric cremated bones? Journal of Archaeological Science 40(1):30–4.

Person A, Bocherens H, Saliège J-F, Paris F, Zeitoun V, Gérard M. 1995. Early diagenetic evolution of bone phosphate: An x-ray diffractometry analysis. Journal of Archaeological Science 22(2):211–21.

Reimer PJ, Brown TA, Reimer RW. 2004. Discussion: Reporting and calibration of post-bomb ^{14}C data. Radiocarbon 46(3):1299–304.

Reimer PJ, Bard E, Bayliss A, Beck JW, Blackwell PG, Ramsey CB, Buck CE, Cheng H, Edwards RL, Friedrich M, Grootes PM, Guilderson TP, Haflidason H, Hajdas I, Hatté C, Heaton TJ, Hoffmann DL, Hogg AG, Hughen KA, Kaiser KF, Kromer B, Manning SW, Niu M, Reimer RW, Richards DA, Scott EM, Southon JR, Staff RA, Turney CSM, van der Plicht J. 2013. IntCal13 and Marine13 radiocarbon age calibration curves 0–50,000 years cal BP. Radiocarbon 55(04):1869–87.

Roehrs H, Klooss S, Kirleis W. 2013. Evaluating prehistoric finds of Arrhenatherum elatius var. bulbosum in north-western and central Europe with an emphasis on the first Neolithic finds in Northern Germany. Archaeological and Anthropological Sciences 5(1):1–15.

Rose HA, Meadows J, Palstra S, Hamann C, Boudin M, Hüls CM. 2019. Radiocarbon dating cremated bone: A case study comparing laboratory methods. Radiocarbon. doi:10.1017/RDC.2019.70.

Snoeck C, Brock F, Schulting RJ. 2014. Carbon Exchanges between bone apatite and fuels during cremation: Impact on radiocarbon dates. Radiocarbon 56(2):591–602.

Snoeck C, Schulting RJ, Lee-Thorp JA, Lebon M, Zazzo A. 2016a. Impact of heating conditions on the carbon and oxygen isotope composition of calcined bone. Journal of Archaeological Science 65:32–43.

Snoeck C, Staff RA, Brock F. 2016b. A reassessment of the routine pretreatment protocol for radiocarbon dating cremated bones. Radiocarbon 58(1):1–8.

Stuiver M, Polach HA. 1977. Discussion: Reporting of ^{14}C data. Radiocarbon 19(3):355–63.

Van Strydonck M, Boudin M, Hoefkens M, De Mulder G. 2005. ^{14}C-dating of cremated bones, why does it work? Lunula. Archaeologia protohistorica XIII:3–10.

Van Strydonck M, Boudin M, De Mulder G. 2009. ^{14}C dating of cremated bones: The issue of sample contamination. Radiocarbon 51(2): 553–68.

Van Strydonck M, Boudin M, Mulder GD. 2010. The carbon origin of structural carbonate in bone apatite of cremated bones. Radiocarbon 52(2):578–86.

Ward GK, Wilson SR. 1978. Procedures for comparing and combining radiocarbon age determinations: A critique. Archaeometry 20(1):19–31.

Zazzo A, Saliège JF, Person A, Boucher H. 2009. Radiocarbon dating of calcined bones: Where does the carbon come from? Radiocarbon 51(2):601–11.

Zazzo A, Saliège JF. 2011. Radiocarbon dating of biological apatites: A review. Palaeogeography, Palaeoclimatology, Palaeoecology 310(1):52–61.

Zazzo A, Saliège J-F, Lebon M, Lepetz S, Moreau C. 2012. Radiocarbon dating of calcined bones: Insights from combustion experiments under natural conditions. Radiocarbon 54(3-4):855–66.

https://doi.org/10.1017/RDC.2020.3 Published online by Cambridge University Press